Available online at www.sciencedirect.com
SCIENCE DIRECT
Journal of Magnetic Resonance 180 (2006) 83–92
JMR Journal of Magnetic Resonance
www.elsevier.com/locate/jmr

Measurement of diffusion in the presence of shear flow

A. Lutti, P.T. Callaghan *

MacDiarmid Institute for Advanced Materials and Nanotechnology, School of Chemical and Physical Sciences, Victoria University of Wellington, Wellington, New Zealand

Received 10 January 2006; revised 17 January 2006
Available online 7 February 2006

Abstract

We demonstrate here a method whereby molecular diffusion coefficients may be measured in the presence of the deformational flow field of a rheo-NMR cell. The method, which uses a repetitive CPMG train of rf pulses interspersed with magnetic field gradient pulses, allows the anisotropic diffusion spectrum to be directly probed. We focus on the cylindrical Couette cell, for which the radial, tangential, and axial directions correspond to the hydrodynamic velocity gradient, velocity, and vorticity directions. While ideal Couette flow does not perturb the vorticity direction, it does perturb diffusion measurements for the velocity gradient direction, and to a lesser extent, the velocity direction. We show that with closely spaced gradient pulses operating in a flow-compensating mode, there exists a diffusion limit below which one cannot measure, that scales as $T^2\dot{\gamma}^4$, where $\dot{\gamma}$ is the shear rate and T the gradient pulse repetition period. For a typical rheo-NMR cell, and for the more challenging velocity gradient direction, diffusion rates above 10^{-12} m^2 s^{-1} can be accurately measured (to 1% error) at shear rates up to 3 s^{-1}. We demonstrate the use of the method in measuring the diffusion spectrum of a lyotropic lamellar phase under shear.

Keywords: Flow; Diffusion; Rheology; Rheo-NMR

1. Introduction

The emerging field of rheo-NMR [1–3] involves not only the mapping of velocity fields but also the measurement of NMR spectroscopic parameters under shear and extensional flow. Such measurements provide unique insight regarding molecular organisation, orientation, and dynamics in the subtle interplay between flow and meso-structural rearrangement. For many NMR parameters, such as relaxation times, chemical shifts, quadrupolar, and dipolar splittings, the presence of shear flow is of no particular concern, although the flow of spin-bearing fluid elements can introduce spectral, or relaxivity perturbation if the magnetic field is insufficiently homogeneous, while rotation of the hydrodynamic axes during circulating flow may confound measurements of molecular orientation by means of quadrupolar or dipolar spectroscopy [4]. This latter phenomenon has been discussed in an earlier paper [5]. In all rheo-NMR endeavours, these potential perturbative effects must be considered and their influences carefully quantified. Generally, their presence will set an upper limit to the shear or extension rates at which phenomena may be investigated.

One particular class of NMR parameter of interest concerns the molecular self-diffusion coefficients associated with the anisotropic diffusion tensor [6–8]. To measure Brownian motion in the presence of a deformational flow field presents a particular challenge. The use of magnetic field gradient pulses in conjunction with spin-echoes to track the diffusive displacements relies on the spin dephasing associated with stochastic motions [9]. However, deformational flow itself causes a separation of molecules which begin in proximity, also leading to a spreading of spin phases over the spin echo. One might approach this problem by ensuring that the echo duration is sufficiently short that no flow effects are present, but of course, this will also reduce the diffusive dephasing. The solution which we

* Corresponding author. Fax: +64 6 350 5164.
E-mail address: Paul.Callaghan@vuw.ac.nz (P.T. Callaghan).

1090-7807/$ - see front matter © 2006 Elsevier Inc. All rights reserved.
doi:10.1016/j.jmr.2006.01.009

demonstrate here is the use of a repetitive train of closely spaced spin echoes, organised in such a way that flow effects are successively cancelled by effective gradient reversal, while the stochastic effects of Brown motion persist, allowing a steady accumulation of phase spreading which arises from diffusion alone [10]. The method allows for the measurement of diffusion in different hydrodynamic directions simply according to the direction of application of the pulses gradients. The pulse sequence tool used is the Carr–Purcell–Meiboom–Gill rf train [11] in which pulses of magnetic field gradient are suitably interspersed. One intriguing aspect of this method is that the time domain of the diffusion measurement is no longer well defined, although there is defined a very special timescale, the cyclic period of the effective gradient waveform. The natural description of this experiment lies in the frequency domain, and the method in fact measures the diffusion spectrum, that is, the spectrum of the velocity autocorrelation spectrum [6,12,13].

The particular rheo-NMR geometry that we consider here is the Couette cell. Rotation of the inner cylinder results in a shearing flow within the annular gap. The natural hydrodynamic axes are velocity (tangential), velocity gradient (radial), and vorticity (axial) as shown in Fig. 1.

Ideally, the rotational flow causes no displacement along the vorticity axis (although deviations from ideality may do so). The particular challenge to be met in measuring molecular self-diffusion will apply to the tangential and radial directions. It is especially interesting to be able to make such measurements. For example, shear flow may induce orientation of meso-phases with respect to the hydrodynamic axes, resulting in anisotropic diffusion. Such diffusion anisotropy may also result from the deformation of molecular aggregates (such as micelles) under flow, as well the deformation of large polymer molecules. Shear flow is also known to induce phase transitions, and to cause the separation of some complex fluids into shear-banded states. In every one of the examples quoted, one might expect a consequential diffusion anisotropy.

Having noted the importance of diffusion measurement in rheo-NMR, and having outlined a method by which such measurement can be achieved, it must be noted that the effect of flow will always be to induce artifacts above some limiting rate-of-strain, unless the gradient waveform period may be arbitrarily shortened. Instrumental limitations will always intervene to place a lower limit on the period, T, of the waveform. In this work, we seek to establish a method whereby the diffusive perturbation may be calculated for any shear rate and any period, giving guidelines for estimating the limits to diffusion measurement in Couette cells. While the method presented here is peculiar to the Couette, it may be easily generalised to other geometries.

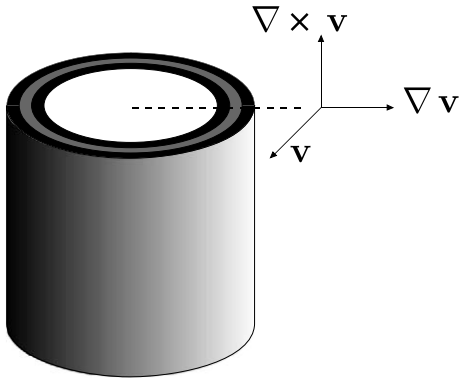

Fig. 1. Velocity (tangential) $\mathbf{v}$, velocity gradient (radial) $\nabla\mathbf{v}$ and vorticity (axial) $\nabla\times\mathbf{v}$, directions for Couette cell with rotating inner cylinder.

2. Theory

2.1. Multi-echo PGSE NMR

Molecular self-diffusion is traditionally measured in NMR by means of the pulsed gradient method of Stejskal and Tanner [9] . A fundamental element of the Pulsed Gradient Spin Echo NMR (PGSE NMR) method is the application of two (oppositely signed) magnetic field gradient pulses of equal amplitude, g, and duration δ separated by an "observation time" Δ. This results in the labelling of the (typically proton) spins with a phase proportional to the gradient amplitude and duration and to the change of position of the water molecules over the observation time. Provided that this motion is purely self-diffusive, the attenuation of the resulting spin-echo signal amplitude can be used to determine the mean-squared displacement of water molecules over the time Δ.

In the case of shear, however, the spin phases contain a contribution arising from the inhomogeneous flow, so that dispersive contributions to the echo amplitude may dominate. Provided that the flow does not change over the duration of the pulse train, this effect can be removed by repeating the pair of encoding gradients [8,10], but with inverted effective polarities (see Fig. 2). The flow contribution to the overall displacement is then compensated leaving only the contribution of the irreversible displacements due to diffusion [10,14]. Where a rotating flow field is employed, as in the Couette cell case to be discussed here, the flow cannot, of course, be constant in any Cartesian sense. Further, there is little purpose in trying to compensate by rotating the gradients [15], since the rotational velocity varies across the annular gap of a Couette cell. Any efficient flow compensation will therefore require the shortest possible time delays between gradient pulses, so that any changes in direction of the local velocities is minimised. This places an upper limit on the longest observation time Δ that may be used at a given shear rate, in turn requiring short duration gradient pulses. This restriction gives little time between the pulses for the spins to diffuse, leading to difficulties in the estimation of the diffusion coefficient. However, by successive repetition of the compensated gradient pulse pairs, sufficient attenuation may be achieved for accurate diffusion coefficient determination [16,17].

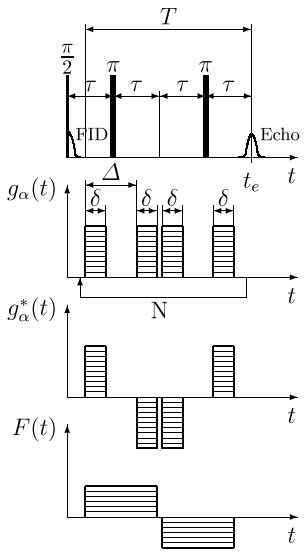

Fig. 2. Multi-echo CPMG gradient train which interspersed gradient pulses. In practice, the centre two pulses are made contiguous so that $\Delta \approx T/2 - \delta$.

In this sense, we may consider the overall effect of an echo train consisting of N periods of alternating gradient pulses, as the successive application of $2N$ Stejskal–Tanner experiments in which the successive stochastic phase spreadings are independent, leading to a total mean-squared phase comprising the sum. In this Gaussian approximation, accurate because of the individually small phase migrations at each gradient pulse pair, the net echo attenuation at the end of the train is given by [12,13,16]:

$$E(g) = \exp\left[-2N\gamma^2\delta^2 g^2 D(\Delta - \tfrac{1}{3}\delta)\right]. \tag{1}$$

Strictly, given finite gradient pulse risetimes (limited by the need to avoid eddy current effects), one needs to take into account the trapezoidal character of the gradient pulses, now taken trapezoidal rather than simply rectangular. The exact expression for the attenuation can thus be deduced from the standard correction to the Stejskal–Tanner expression [18],

$$E(g) = \exp\left[-2N\gamma^2 g^2 D\left\{\delta'^2(\Delta - \tfrac{1}{3}\delta') + \frac{\varepsilon^3}{30} - \frac{\delta'\varepsilon^2}{6}\right\}\right], \tag{2}$$

where $\delta' = \delta + \varepsilon$, δ being the duration of the gradient pulse maximum and ε the pulse rise and fall time. Henceforth we shall, for simplicity, write the product $\gamma^2 g^2\{\delta'^2(\Delta - \frac{1}{3}\delta') + \frac{\varepsilon^3}{30} - \frac{\delta'\varepsilon^2}{6}\}$ as $q^2\Delta_{\text{eff}}$, although the exact expression will always be implied.

2.2. The diffusion spectrum

While Eqs. (1) and (2) provide an accurate means of measuring the apparent diffusion coefficient, D, the interesting question arises as to how we should interpret this quantity, and in particular, what timescale we should attribute to its measurement. First, we should strictly write it as the diagonal element of the diffusion tensor [6], $D_{\alpha\alpha}$ where the subscript α refers to either the velocity, gradient or vorticity direction. In fact, the quantity measured is the element of the diffusion tensor spectrum, $D_{\alpha\alpha}(\omega)$, at the angular frequency, $2\pi/T$. This interpretation is made possible as described in various papers by Stepisnik et al [12,13,16,19]. The CPMG multi-echo PGSE NMR experiment has been demonstrated and analysed by Callaghan and Stepisnik [16] and used in a number of applications [16,17,20]. The multi-echo train imparts successive attenuations to the echoes, and is sensitive to the details of the diffusive process through the periodic excursions of the spin phases caused by the successive, oppositely signed, gradient pulse pairs. The rf/gradient train can be represented by a pure effective gradient train [12], $g^*(t)$, the successive sign of the effective gradient being alternated by the effect of the rf pulses (see Fig. 2). The fundamental period of this effective gradient train is written T and its effect is best analysed in the frequency domain of the motion, using the frequency characteristics of the periodic gradient pulse train. For a train of many periods, i.e., with total duration much longer than T, the train has narrow spectrum of characteristic cyclic frequency $1/T$.

In the Stepisnik description [12], the echo attenuation of the gradient train is written as:

$$E = \exp\left[-\frac{\gamma^2}{2\pi}\int_{-\infty}^{\infty}|F(\omega)|^2 D_{\alpha\alpha}(\omega)\,\mathrm{d}\omega\right], \tag{3}$$

where $F(\omega) = \int_0^\infty F(t)\mathrm{e}^{i\omega t}\,\mathrm{d}t$ and $F(t) = \int_0^t g*(t')\mathrm{d}t'$. The diffusion spectrum, in this context, is simply the Fourier transform of the molecular velocity autocorrelation function [6],

$$D_{\alpha\alpha}(\omega) = \int_0^\infty < v_\alpha(0)v_\alpha(t) > \mathrm{e}^{-i\omega t}\,\mathrm{d}t, \tag{4}$$

where α is one of the (chosen) axis directions, x, y or z.

Eq. (3) indicates that the experiment is sensitive to the region of the diffusion spectrum sampled by the frequency characteristic of the gradient sequence. More precisely, for an N period multi-echo train,

$$|F(\omega)|^2 = \left(\frac{2\gamma g\delta}{\omega}\right)^2 \frac{\sin^2(N\omega T/2)}{\cos^2(\omega T/2)}\sin^2(\omega T/8). \tag{5}$$

The essential features of Eqs. (3) and (5) are shown in Fig. 3. The effective gradient spectrum consists of one main lobe centered at $\omega = 2\pi/T$. It is therefore possible to measure the diffusion spectrum by appropriately varying the period of the NMR sequence. Of course, the frequency dependence of the diffusion spectrum depends on the details of molecular displacement fluctuations in the system under study.

2.3. The diffusion measured for a sheared fluid in a Couette cell

The rapid application of alternating sign effective gradient pulses causes coherent motion to be removed. However

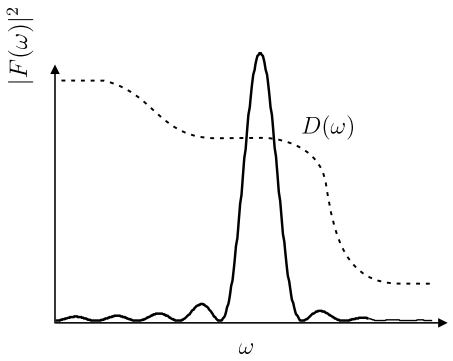

Fig. 3. Schematic effective gradient spectrum used to sample the diffusion spectrum $D(\omega)$.

changes in coherent motion will contribute to phase shifts whose size diminishes as the period of gradient sign alternation reduces. In a Couette cell, where diffusion is to be measured in the flow-gradient plane (i.e., tangential and radial to the flow), there will always be a finite phase shift arising from coherent motion change because of the rotational nature of the flow. Further, because the angular speed of that rotation changes across the annular gap in shear flow, the application of rotating gradients in an attempt to avoid that phase change, can only work for one singular radial point in the gap. We shall show, however, that for any known periodicity, rotation rate, and expected diffusion coefficients, the bounds over which the modulated gradient train gives an accurate result, may be clearly defined. Indeed, we show that for practical values of the alternation period (for example, around 10 ms) anisotropic diffusion, over the range 1–0.001 D_{water} may be practically measured in a 1 mm gap at shear rates up to 3 s^{-1}. The theory presented here enables the experimenter to determine limits for any experimental situation.

The principle behind our calculation method is shown in Fig. 4. Ideally, the alternating sign effective gradient train is applied via a CPMG sequence of rf pulses, with four identical infinitesimally narrow gradient pulses, applied at times $(0, T/2, T/2, T)$ over the cycle period T, with a total of N cycles being used over the entire evolution time of the train. With finite pulses, of duration δ, the commencement of the pulses is at $(0, T/2-\delta, T/2, T-\delta)$. In the slice selection experiment which we use (see Fig. 4), the train is immediately followed by a slice selection rf pulse which is used to define the region of the Couette cell from which the signal is to be acquired. To find the signal amplitude we must integrate across the gap, allowing for the local radially dependent signal phase encoding over the entire history of the pulse sequence.

There are two parts to the calculation. The first takes account of flow only, which is assumed to be laminar, and, for the purposes of this exercise, the flow profile $v(r)$, with angular equivalent $\omega(r)$, associated with a Newtonian fluid. It is however a trivial matter to carry out the following calculation with any known flow profile. Note that at each radius, the fluid element to be detected in the

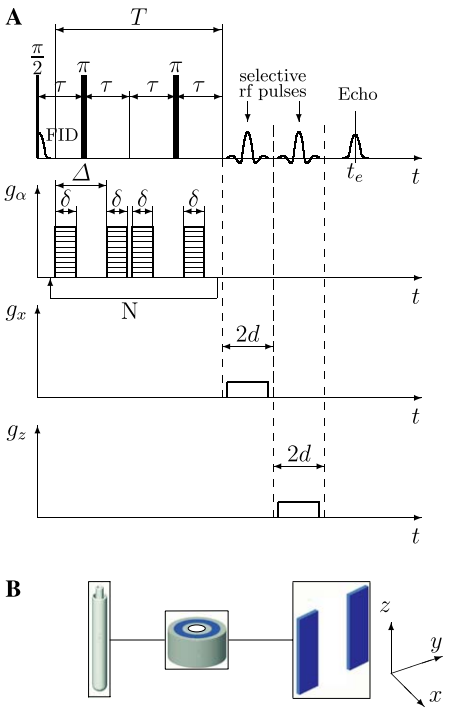

Fig. 4. (A) Multi-pulsed gradient spin echo experiment in which a repetitive train of repeated four diffusion-encoding gradient pulses is followed by slice selective rf/gradient pulse combinations. Note that the two pairs of gradient pulses depicted have opposite effective sign for motion encoding. The diffusion-encoding gradient, g_α may be applied along any of the Cartesian axes. (B) Selective excitation enables measurement on a chosen slice.

final slice selection, has been encoded over a history of prior locations, described by a local azimuthal angle $\theta(t)$. The second part takes account of the locally anisotropic diffusion. Here, each quadruplet of gradient pulses in the cycle results in an attenuation factor, depending on the local azimuthal orientation of that radial fluid element at each cycle step in the prior history.

2.3.1. The flow contribution

We begin by writing the radial dependence of angular velocity for Newtonian flow between the inner cylinder of outer radius r_1, with wall angular speed $\omega(r_1)$ and the outer cylinder with inner radius r_2 and angular speed zero. A no slip condition is assumed,

$$\omega(r) = \omega(r_1)\left(\frac{r_2^2}{r^2} - 1\right)/\left(\frac{r_2^2}{r_1^2} - 1\right). \tag{6}$$

For any element of fluid at radius r, its azimuthal angle with respect to the slice location at time t before slice selection and detection is given by (see Fig. 5):

$$\theta(t) = \omega(r)(NT - t). \tag{7}$$

Note that the inclusion of the (usually short) time of selection is straightforward and represents a minor perturbation in the analysis. Note further that slice selection generally results in signal acquisition from two regions of the annulus separated by angle π.

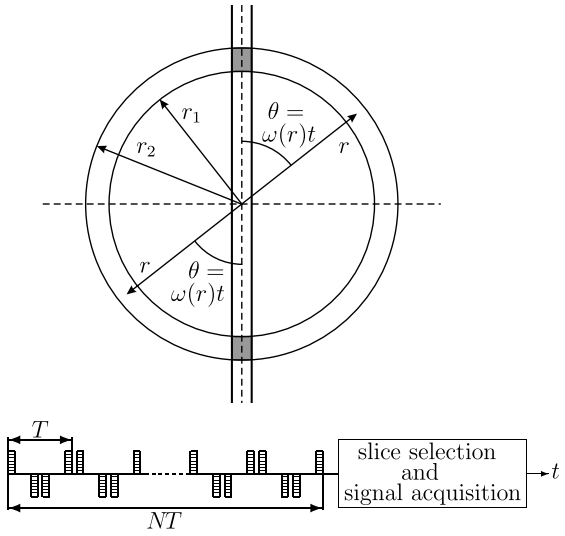

Fig. 5. Local azimuth of fluid to be ultimately detected in the chosen slice, at a prior time before slice selection and during gradient encoding for motion.

For each gradient pulse of area q (i.e., $g\delta$), the locally acquired phase factor is $\exp(iqr\sin(\theta(t))$ for tangential diffusion measurements (x-encoding) and $\exp(iqr\cos(\theta(t))$for radial diffusion measurements (y-encoding), as shown in Fig. 5. For the nth gradient pulse period ($n = 1$–N), the local time for commencement of each of the four component gradient pulses is $t = nT - T$, $nT - T/2 - \delta$, $nT - T/2$, $nT - \delta$ with corresponding signs of the phase factor exponents, $+,-,-,+$.

Allowing for signal contributions from both slice arcs at opposite sides of the Couette cell, and assuming a narrow gap the flow contribution to the normalised signal attenuation, for the respective cases of tangential (x-gradient pulses) and radial (y-gradient pulses) is given by:

$$E_t(q) = \frac{1}{r_2 - r_1}\int_{r_1}^{r_2} \cos\left(4qr\sin\left(\omega(r)\left[\frac{1}{4}T - \frac{1}{2}\delta\right]\right)\right. \times \sin\left(\omega(r)\frac{1}{4}T\right)\left.\sum_{n=1}^{N}\sin\left(\omega(r)\left(N - n + \frac{1}{2}T\right)\right)\right)\mathrm{d}r,$$

$$E_r(q) = \frac{1}{r_2 - r_1}\int_{r_1}^{r_2} \cos\left(4qr\sin\left(\omega(r)\left[\frac{1}{4}T - \frac{1}{2}\delta\right]\right)\right. \times \sin\left(\omega(r)\frac{1}{4}T\right)\left.\sum_{n=1}^{N}\cos\left(\omega(r)\left(N - n + \frac{1}{2}T\right)\right)\right)\mathrm{d}r, \quad (8)$$

Note that use excitation of a semi-rectangular arc by the slice selection rf pulses dictates the integration over dr, and not $2\pi r\mathrm{d}r$. The summation term takes account of the azimuthal angular displacement away from the ideal orientation, during the N prior gradient pulse cycles, the radial attenuation being more severely affected by this artifact. The $\sin(\omega(r)\frac{1}{4}T)$ term arises from the change in fluid element flow orientation during those cycles. It expresses the capacity of the four pulse cycle to compensate the changes in velocity during rotational flow.

2.3.2. The diffusive contribution

Of course, Eq. (8) represents the effective signal attenuation in the absence of diffusion. Suppose now that superposed on the flow is an anisotropic molecular diffusion (D_t, D_r). It is these two values that we seek to measure. Thus, one would hope that the attenuation due to diffusion will significantly outweigh that due to flow artifacts. Note that again, the existence of an azimuthal angular offset during the prior gradient pulse train induces a potential artifact, namely the tendency to admix tangential and radial diffusion components. Each quadruple (i.e., cyclic period) of gradient pulses applied along the x-axis imparts, for a fluid element at radius r, an attenuation $\exp(-q^2\cos^2(\omega(r)(N-n)T)D_tT + \sin^2(\omega(r)(N-n)T)D_rT)$ giving a total attenuation, at that radius, of

$$E(D_t, D_r, r) = \exp\left(-q^2\left[\sum_{n=1}^{N}\cos^2(\omega(r)(N-n)T)D_tT + \sin^2(\omega(r)(N-n)T)D_r\right]T\right). \quad (9)$$

For slow angular speeds, this reduces to $\exp(-q^2ND_tT)$, the ideal result. When the gradient is applied along the y-axis then the same expression applies but with D_t and D_r interchanged. Thus, combining Eqs. (8) and (9), we find

$$E_t(q) = \frac{1}{r_2 - r_1}\int_{r_1}^{r_2} E(D_t, D_r, r) \times \cos\left(4qr\sin\left(\omega(r)\left[\frac{1}{4}T - \frac{1}{2}\delta\right]\right)\sin\left(\omega(r)\frac{1}{4}T\right)\right. \times \left.\sum_{n=1}^{N}\sin\left(\omega(r)\left(N - n + \frac{1}{2}T\right)\right)\right)\mathrm{d}r,$$

$$E_r(q) = \frac{1}{r_2 - r_1}\int_{r_1}^{r_2} E(D_t, D_r, r) \times \cos\left(4qr\sin\left(\omega(r)\left[\frac{1}{4}T - \frac{1}{2}\delta\right]\right)\sin\left(\omega(r)\frac{1}{4}T\right)\right. \times \left.\sum_{n=1}^{N}\cos\left(\omega(r)\left(N - n + \frac{1}{2}T\right)\right)\right)\mathrm{d}r. \quad (10)$$

We will use these equations to determine the effective diffusion coefficient by comparing the calculated attenuation with that given by Eq. (1). Further, by setting the real diffusion coefficients, D_t and D_r to zero, and ascertaining the apparent perturbative diffusion coefficients predicted by Eq. (10), we are able to establish scaling laws for dependence of this perturbation on T and the shear rate $\dot{\gamma}$. However, we are also able to deduce this effect in a slightly simplified analysis as follows.

2.3.3. Simplified analysis

In the treatment above, the progressive azimuthal displacements of the fluid during the gradient pulses is accounted for. A simpler description results if we

consider an element of fluid, in the chosen slice, from the perspective of one single four gradient pulse period, then simply multiply successive attenuations, assuming that all fluid elements remain fixed. This treatment allows us to ascertain the scaling laws governing the dependence on apparent diffusive perturbation on T and $\dot{\gamma}$ and is quite accurate providing the angular excursions remain small ($\omega nT \ll \pi$).

Consider the attenuation arising from an single cycle of 4 gradient pulses applied in the direction α. The first pair record a velocity v_α and the second, v'_α resulting in a phase factors dependent on the change of velocity Δv_α. Allowing that the attenuation will be small, we may use the cumulant expansion to write the echo attenuation factor as

$$\langle \exp(iq\Delta v_\alpha \Delta)\rangle = \exp(iq\langle \Delta v_\alpha\rangle \Delta) \times \exp\left(-\tfrac{1}{2}q^2\left\{\langle \Delta v_\alpha^2\rangle - \langle \Delta v_\alpha\rangle^2\right\}\Delta^2\right), \quad (11)$$

where the angular brackets incorporate integration over the entire sample region represented by the excited slice. Allowing for the contribution of slice segments at 180° opposition we find $\langle \Delta v_\alpha\rangle = 0$. The effective diffusion coefficient arising from Eq. (11) is determined by noting that for the four gradient pulses cycle diffusive attenuation should be given by $\exp[-2q^2 D_{\text{app}}\ (\Delta - \delta/3)]$ leading to

$$D_{\text{flow}} = \frac{< \Delta v_\alpha^2 > \Delta^2}{4\Delta_{\text{eff}}}. \quad (12)$$

For the tangential direction ($\alpha = x$) the value of Δv_x in the case of the Couette cell at all radii is zero to first order, because of symmetry. For the radial direction velocity ($\alpha = y$) Δv_y at any radius r in the annulus may be calculated from a knowledge of the local angular velocity, namely $\Delta v_y = r\omega(r)^2\Delta$. In terms of the angular speed of the inner cylinder, the inner and outer radii of the gap, we find, for Newtonian flow [21],

$$\Delta v_y^2(r) = \frac{\Delta^2\omega^4 r^2}{(r_2^2 - r_1^2)}\left[\frac{r_2^2 - r^2}{r^2}\right]^4. \quad (13)$$

Integrating Δv_y^2 over the gap to obtain $< \Delta v_y^2 >$, allowing $\Delta = T/2$, we find

$$D_{flow} = kT^3\dot{\gamma}^4, \quad (14)$$

where k is a function of r_1, r_2, and ω obtained from the gap integral.

It should be noted that this contribution to the apparent diffusion coefficient from the flow will add to the true self-diffusion coefficient arising from Brownian motion. This the condition that the flow contribution should be insignificant amounts to $D_{\text{flow}} \ll D_{\text{Brownian}}$. While the major influence of flow will be on the radial component of diffusion, the finite angular displacement which occur during the CPMG encoding also lead to a weaker perturbation to the tangential component. This latter effect is accounted for in Eq. (10).

Finally, we test our multi-echo train in the measurement of diffusion in a simple fluid under shear and then we apply it to the measurement of anisotropic diffusion in a lamellar phase lyotropic liquid crystal, showing that we are able to accurately measure diffusive behaviour up to the maximum shear rate of 15 s^{-1}.

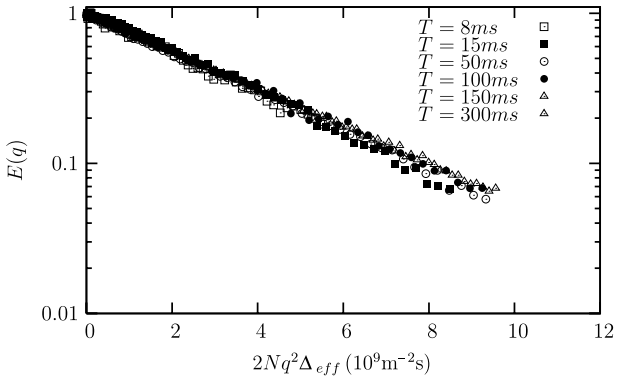

Fig. 6. Multi-echo CPMG sequence measurements of (radial) echo attenuation for pentanol under zero shear rate, showing the independence of diffusion coefficient on waveform period.

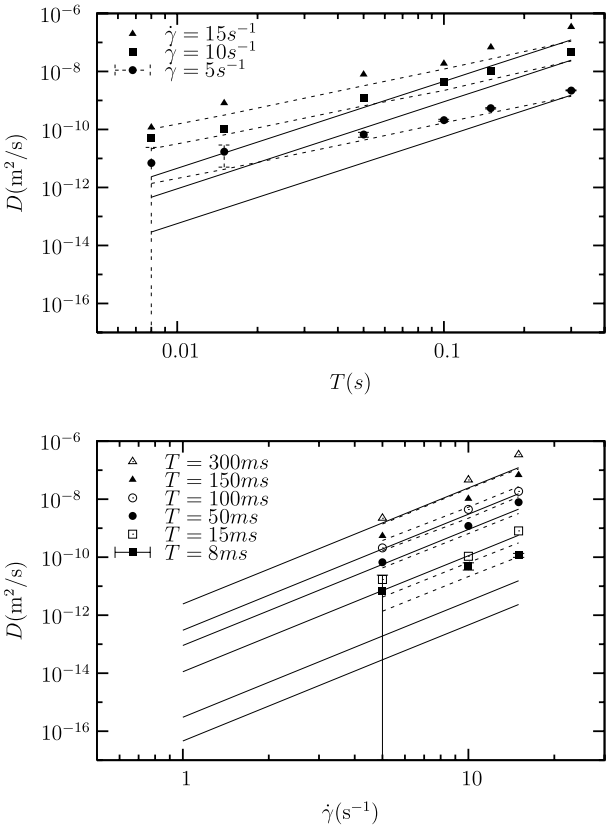

Fig. 7. Flow contribution to apparent diffusion (radial encoding) for various values of the strain rate and the CPMG period time, T for which the total encoding time is 300 ms, considerably longer than used in the experiments reported in Fig. 11. Except where shown, the error bars in the measurements are on the order of or smaller than the symbol size. The dashed line is for "exact" model of Eq. (8). The solid line is for the simplified analysis represented by Eq. (14) and does not take account of the changing azimuthal angle over the encoding period.

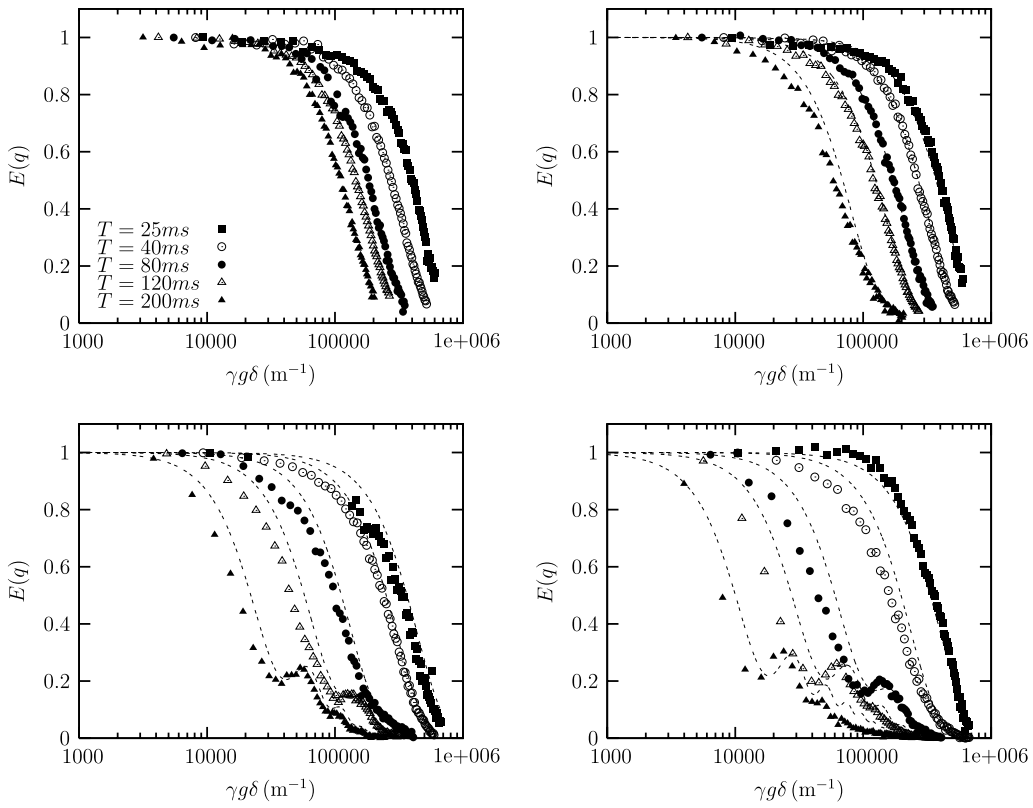

Fig. 8. Theoretical and experimental echo attenuations for pentanol at various shear rates, increased from left to right, top to bottom as 1 s^{-1}, 5 s^{-1}, 10 s^{-1} and 15 s^{-1} and for various gradient pulse periods, T, as shown, for the case of a single four pulse train.

Table 1
Comparison of q_{min} values for oscillatory echo attenuation decays, as predicted by the simple "flow diffraction" picture of the gap-averaged Fourier spectrum of the probability distribution, and those vales seen experimentally

$\dot{\gamma}$ (s^{-1})	$T = 80$ ms; $\Delta = 37.17$ ms		$T = 120$ ms; $\Delta = 57.07$ ms		$T = 200$ ms; $\Delta = 97.07$ ms	
	q_{min} (theor)	q_{min} (exp)	q_{min} (theor) [m^{-1}]	q_{min} (exp) [m^{-1}]	q_{min} (theor) [m^{-1}]	q_{min} (exp) [m^{-1}]
10	—	—	8.6×10^4	10×10^4	2.9×10^4	3.2×10^4
15	9.3×10^4 m^{-1}	10×10^4 m^{-1}	3.8×10^4	4.2×10^4	1.3×10^4	1.3×10^4

3. Experiment

A test of the effectivenes of the CPMG gradient pulse train in measuring diffusion in the presence of shear was carried out using a sample of pentanol (Aldrich, Castle Hill, NSW, Australia)) for which the diffusion coefficient is 2.9×10^{-10} m^2 s^{-1} at 22 °C.

All measurements were carried out at 22 °C using a Bruker Avance 300 MHz NMR spectrometer, using the three-axis magnetic field gradients of the Micro2.5 probe. Shear is applied using a Couette cell made of two concentric glass NMR tubes of 16 mm (OD) and 18 mm (ID), respectively. The Couette cell vorticity axis is aligned parallel to the (vertical) direction of the polarizing magnetic field. The inner cylinder can be rotated within the NMR spectrometer by means of a specially constructed shaft and stepper-motor-gearbox drive.

In our experiment we wish to select a small arc of the Couette cell so that the velocity and gradient directions are well defined. This is achieved by means of two "slice-selective" radiofrequency pulses applied in combination with magnetic field gradients. One slice (thickness 30 mm) is taken perpendicular to the longitudinal (vorticity) axis of the Couette cell and defines the longitudinal section to be averaged. The other slice (thickness 3 mm) is taken perpendicular to a diametral direction. This choice of selected sample volume defines a simple three-dimensional cartesian system along which one can apply the diffusion-encoding gradients. These correspond to the directions x (tangential = velocity direction ($\mathbf{v}$), y (radial = velocity gradient direction ($\nabla\mathbf{v}$) and z (longitudinal = vorticity direction ($\nabla \times \mathbf{v}$). Angular velocities are varied to provide shear rates ranging from 10^{-2} to 15 s^{-1}. In all diffusion experiments, the NMR signal was detected using the proton nucleus.

Each experiment is carried out at fixed N and T by varying the gradient amplitude, g. By this means, relaxation effects are normalised. Fig. 6 shows a set of calibration

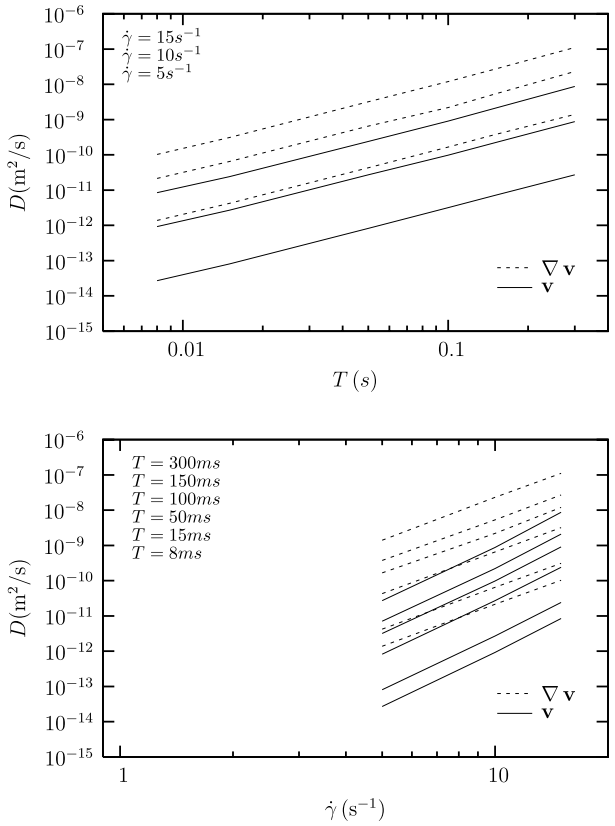

Fig. 9. Flow contributions to apparent diffusion calculated using Eq. (8), for encoding in the radial (dashed lines) and tangential (solid lines) for a range of shear rates and cycle periods, for the case of the cylindrical Couette cell used in this work.

measurements on pentanol over a variety of periods T, but with NT fixed at around 300 ms.

The system studied here is 30% w/w cetylpyridinium chloride and hexanol diluted in brine (1% w NaCl). All materials were purchased from Sigma–Aldrich. Samples were prepared at room temperature and allowed to equilibrate for one week before use. The mass ratio hexanol/CpCl is taken from the phase diagram [22] and at 0.92 is designed to provide a lamellar phase remote from any phase boundaries.

4. Results

4.1. Flow artifacts for radial measurement

Below 5 s^{-1}, measurement of the diffusion coefficient of pentanol was sufficiently accurate, that no flow contribution was able to be ascertained, independent of the period of the gradient pulse train used. At shear rates above 5 s^{-1}, the accurate measurement of pentanol diffusion in the radial direction depends on the use of a short period gradient train. The flow contribution to pentanol diffusion, is measured by subtracting the known (measured at zero shear) pentanol diffusion coefficient from that measured under shear using a train of gradient pulses of total duration, $NT = 300$ ms. This is a rather long encoding time compared with most practical measurements and is chosen to deliberately exaggerate the flow contribution to diffusion.

To test the ability of both the simple theory and the more exact treatment of Eq. (10) to represent the data we show, in Fig. 7, the dependence of the radial component of D_{flow} on both shear rate and cycle period, T. There is noticeable agreement between the exact model theoretical predictions (Eq. (8)) and the data obtained by observing the artifactual enhancement the observed pentanol diffusion coefficient. By contrast, the simple scaling law of Eq. (14) breaks down since it fails to allow for the effect of the changing azimuthal angle over the encoding period a T is increased. Eq. (14) does however appear to correctly represent the scaling of D_{flow} with shear rate.

It is interesting to consider how accurately one could measure a radial diffusion coefficient of $1 \times 10^{-10}\,\mathrm{m}^2\,\mathrm{s}^{-1}$ given the effect of D_{flow}. Note that at $T = 100$ ms, the perturbation for 5 s^{-1} is around a factor of 3 whilst for 15 s^{-1}it is a factor of 200. By contrast at $T = 8$ ms, the measurement is accurate to 10% error at all shear rates up to 5 s^{-1} while it is perturbed by a factor of 2 at 15 s^{-1} (see Fig. 7). By choosing a shorter total encoding period, NT, these errors may be considerably reduced.

An exceptionally sensitive test of the theory applies at the highest strain rates and at long periods, T. In this region, a gaussian behaviour for the echo attenuation following Eq. (1) (i.e., attenuation as a semlogarithmic dependence on q^2) is no longer observed. In seeking to represent the echo attenuation data for a finite value of solvent diffusion, Eq. (10) should be capable of predicting the shape at finite q values at all values of shear rate and period time T.

Using a single period echo train we seek to investigate this behaviour. Remarkably, an oscillatory echo decay is observed (see Fig. 8), an effect displayed clearly by plotting the echo amplitude versus $\log q$. The set of experiments shown were performed using a single four pulse gradient cycle of duration T, varying T for different shear rates. The agreement between the data and the predictions of Eq. (10) are sufficiently close to give one confidence in the analysis. It should be noted that very small deviations from the Newtonian flow profile assumed here can cause a distinct change in the oscillatory echo behaviour. One intriguing aspect is the influence of Taylor dispersion, which we have not accounted for here. The RMS displacements across streamlines over the longest period cycle of 200 ms would be on the order of 10 μm, probably insufficient to cause a major deviation from ideal Newtonian behaviour for the 1 mm gap employed here.

Note that we may gain some intuition regarding the oscillation in the echo attenuation by considering the gap-averaged Fourier spectrum of the probability distribution for change in velocity over the effective gradient period. This suggests an oscillatory behaviour represented by $\mathrm{sinc}\left(\frac{q}{2}\frac{(\Delta r_1^2\omega_1)^2}{(r_2+r_1)(r_2^2-r_1^2)}\right)$, an expression which suggests an echo

minimum at $\frac{q_{\min}}{2}\frac{(\Delta_1^2\omega_1)^2}{(r_2+r_1)(r_2^2-r_1^2)}=\pi$. Table 1 compares observed minimum q values with those suggested by this analysis. The agreement is good.

4.2. Comparative Flow artifacts for radial and tangential measurement

Fig. 9 shows the predictions of Eq. (10) for the dependence of the artifactual D_{flow} versus T and $\dot{\gamma}$ calculated by setting the true molecular diffusion coefficients, $D_t = D_r = 0$. It is clear that at sufficiently low shear rates and period times, these follow the approximate scaling laws

$$D_{flow}^{\nabla v} \sim T^2\dot{\gamma}^4,$$
$$D_{flow}^{v} \sim T^2\dot{\gamma}^6. \quad (15)$$

Note that the quadratic T scaling found here differs from the cubic of the simple model where the effect of azimuthal reorientation is ignored.

It should be noted that one of the consequences of the azimuthal angle deviation during the echo train gradient encoding prior to slice selection, is that the radial and tangential directions become admixed. This may inhibit the measurement of diffusion anisotropy. Indeed, for correct measurements of anisotropy by a factor $\eta = D_r/D_t$ one requires that the sine of the maximum prior excursion angle should be small ($\sin^2(\omega(r)NT) < \eta$). This condition is easily satisfied in the application which we show next, namely, the measurement of anisotropic diffusion in a lamellar liquid crystal.

4.3. Anisotropic diffusion in a lamellar phase under shear

Fig. 10 shows the diffusion spectrum measured at zero shear in the lamellar system CPyCl/hexanol/brine. A detailed analysis of the low shear rate dependence of the diffusion spectrum has been published elsewhere [23].

In Fig. 11, we show a succession of high frequency (short T) diffusion coefficients for both the radial and tangential components, at shear rates of 0.05 s^{-1}, 5 s^{-1}, and 15 s^{-1}. In these measurements, the total encoding time, NT, was around 100 ms The gradual loss of anisotropy is probably due to a conversion of the lamellar phase to the onion phase under shear. Using Eq. (10) we are able to predict the flow contribution to the echo attenuation, and these are shown as straight lines in Fig. 11. It is clear that the experimental measurements are not significantly perturbed given the parameters used in these measurements.

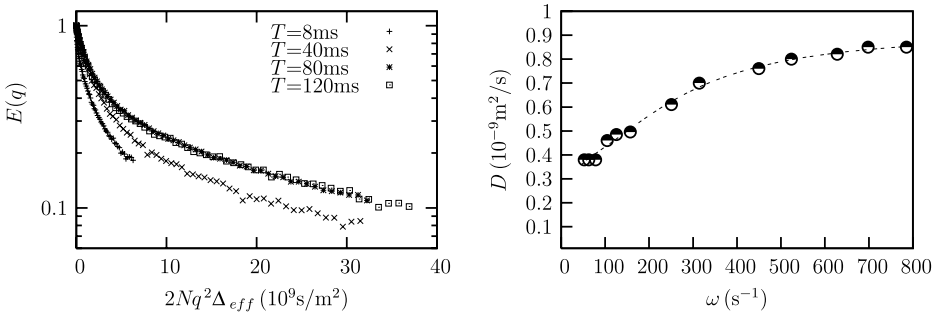

Fig. 10. Attenuation of the signal due to the diffusion of water molecules within lamellar bilayers of CPyCl/hexanol/brine at zero shear. The gradient is applied in the radial direction. The changes in the initial slope of the echo attenuation data yield the diffusion spectrum shown on the right.

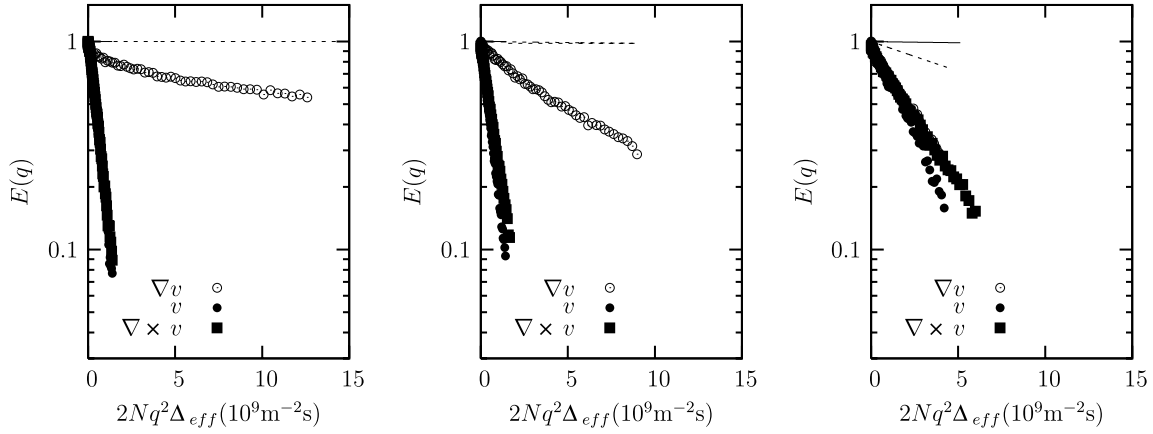

Fig. 11. Attenuation of the (radial and tangential) signals due to the diffusion of water molecules within lamellar bilayers of CPyCl/hexanol/brine as the shear rate is increased successively (left to right) from 0.05 s^{-1} to 5 s^{-1} to 15 s^{-1}. Note the decreasing anisotropy as the lamellar to onion state transition occurs. The flow effect on diffusion measurement is weak, as indicted by the dashed (radial) and solid (tangential) lines, and only at 15 s^{-1} is does the influence of flow effects begin to be seen on the radial diffusion.

5. Conclusions

The theory presented here for describing the perturbative effect of flow on diffusion measurements in the presence of shear, is particular to the CPMG multi-gradient pulse train, and the Newtonian flow field of the Couette cell. However, we assert that such calculations could be easily reproduced for other geometries and flow fields. Certainly, we have shown that it is quite straightforward to measure diffusion coefficients in excess of $10^{-10}\,m^2\,s^{-1}$ for shear rates below $10\,s^{-1}$. Of course these calculations apply to a 1 mm gap. It is possible to achieve diffusion measurement accuracy at considerably higher shear rates if the Couette cell gap is reduced, and especially if the effective gradient period time T is further reduced.

It is tempting to consider the prospect of correcting the apparent diffusion coefficient for flow effects under known conditions. We assert that this is exceedingly difficult because of the high sensitivity of the artifactual echo attenuation on the exact details of the flow field, and even small deviations from Newtonian behaviour can have a marked effect. However, it is perfectly clear that one may calculate the experimental regime in which accurate measurements can be safely performed, given a rudimentary knowledge of the flow behaviour.

A particularly interesting question concerns the practical lower limits to the period T of the effective gradient period time, given the dependence of D_{flow} on T^2. We have found it difficult to reduce below $T = 8$ ms, because of rise time effects and the limited gradient strength. Any major improvement in gradient technology relating to these limits may considerably extend the use of diffusion anisotropy measurements to higher shear rates than those reported here.

Acknowledgments

The authors would like to acknowledge grant support from the New Zealand Foundation for Research, Science and Technology and the Royal Society of New Zealand Marsden Fund and Centres of Research Excellence Fund. We are grateful to Kate McGrath for advice concerning the lyotropic phase used here.

References

[1] P.T. Callaghan, Rheo-NMR: nuclear magnetic resonance and the rheology of complex fluids, Reports Prog. Phys. 62 (1999) 599–670.
[2] M.M. Britton, P.T. Callaghan, M.L. Kilfoil, R.W. Mair, K.M. Owens, NMR velocimetry at microscopic resolution in small rheometric devices, Appl. Magn. Reson. 15 (1998) 287–301.
[3] P.T. Callaghan, Rheo-NMR: a new window on the rheology of complex fluids, Encyclopedia Magn. Reson. 9 (2002) 739–750.
[4] R.J. Cormier, M.L. Kilfoil, P.T. Callaghan, Bi-axial deformation of a polymer under shear: NMR test of Doi-Edwards model with convected constraint release, Phys. Rev. E 6405 (2001) 1809.
[5] J.M. Atkin, R.J. Cormier, P.T. Callaghan, Effects of angular displacements on ^{2}H NMR spectra for deformed polymers under shear, J. Magn. Reson. 172 (2005) 91–97.
[6] R. Kubo, M. Toda, N. Hashitsume, Statistical Physics II, Springer-Verlag, Berlin, 1978.
[7] P.J. Basser, J. Mattielo, D. Lebihan, MR diffusion tensor spectroscopy and imaging, Biophys. J. 66 (1994) 259–267.
[8] P.T. Callaghan, Principles of Nuclear Magnetic Resonance Microscopy, OUP (Oxford, 1991).
[9] E.O. Stejskal, J.E. Tanner, Spin diffusion measurements: spin echoes in the presence of a time-dependent field gradient, J. Chem. Phys. 42 (1965) 288–292.
[10] P.T. Callaghan, S.L. Codd, J.D. Seymour, Spatial coherence phenomena arising from translational spin motion in Gradient Spin Echo experiments, Concept Magnetic Reson. 11 (1999) 181–202.
[11] H.Y. Carr, E.M. Purcell, Effect of diffusion on free precession in Nuclear Magnetic Resonance experiments, Phys. Rev. 94 (1954) 630–638.
[12] J. Stepisnik, Analysis of NMR self-diffusion measurements by a density matrix calculation, Physica B 104 (1981) 350–364.
[13] P.T. Callaghan, J. Stepisnik, Generalised analysis of motion using magnetic field gradients, Adv. Magn. Opt. Reson. 19 (1996) 325–388.
[14] S.L. Codd, B. Manz, J.D. Seymour, P.T. Callaghan, Taylor dispersion and molecular displacements in Poiseuille flow, Phys. Rev. E 60 (1999) R3491–R3494.
[15] A.J. Sederman, K.G. Hollingsworth, M.L. Johns, L.F. Gladden, Development and application of rotationally compensated RARE, J. Magn. Reson. 171 (2004) 1180123.
[16] P.T. Callaghan, J. Stepisnik, Frequency domain analysis of spin motion using modulated gradient NMR, J. Magn. Reson. A117 (1995) 118–122.
[17] P.T. Callaghan, S.L. Codd, Flow Coherence in a bead pack observed using Frequency Domain Modulated Gradient NMR, Phys. Fluids 13 (2001) 421–427.
[18] C.M. Trotter, PhD thesis, Massey University, 1981 (unpublished); W.S. Price, P.W. Kuchel, Effect of non-rectangular field gradient pulses in the Stejskal and Tanner (diffusion) pulse sequence), J. Magn. Reson. 94 (1991) 133–139.
[19] J. Stepisnik, P.T. Callaghan, The long time tail of molecular velocity correlation in a confined fluid: observation by modulated gradient spin-echo NMR, Physica B 292 (2000) 296–301.
[20] J. Stepisnik, A. Mohoric, A. Duh, Diffusion and flow in a porous structure by the gradient spin echo spectral analysis, Physica B 307 (2001) 158–168.
[21] T.E. Faber, Fluid Dynamics for Physicists, Cambridge University Press, Cambridge, 1995.
[22] H.F. Mahjoub, K.M. McGrath, M. Kleman, Phase transition induced by shearing of a sponge phase, Langmuir 12 (1996) 3131.
[23] A. Lutti, P.T. Callaghan, Undulations and fluctuations in a lamellar phase lyotropic liquid crystal and their suppression by weak shear flow, Phys. Rev. E (in press).